Journal of Sound and Vibration (2001) **239**(1), 19–39
doi:10.1006/jsvi.2000.3110, available online at http://www.idealibrary.com on IDEAL®

SUPER-ELEMENT WITH SEMI-RIGID JOINTS IN MODEL UPDATING

S. S. LAW, T. H. T. CHAN AND D. WU

Department of Civil Structural Engineering, Hong Kong Polytechnic University, Hung Hom, Kowloon, Hong Kong. E-mail: cesslaw@polyu.edu.hk

(*Received* 25 *January* 2000, *and in final form* 19 *May* 2000)

Civil engineering structures usually consist of a large number of members connected by joints. The joints are fixed with different types of fasteners, and they provide a certain amount of flexibility towards the static and dynamic behavior of the structure. Model updating of such a structure in practice is to improve the substructures followed by the joint property identification. This paper presents a method to update a super-element model of such a structure. The parameter selection strategy of *generic* element is adopted and the joint stiffnesses are treated as generic parameters to be updated simultaneously together with other structural parameters. An experiment with a three-dimensional steel truss is studied to illustrate the efficiency of the proposed method.

1. INTRODUCTION

A remarkable number of methods for updating the analytical model of structures have been developed in the last few decades, as discussed in a survey paper by Mottershead and Friswell [1]. Among them, there are broadly two categories of updating methods: *direct method* and *parameter method*.

The direct methods or the matrix methods will always produce an updated model which replicates the measured data exactly, and the Lagrange multiplier and matrix mixing approaches have the advantage of computational efficiency compared to other methods. However, these methods do not provide any mechanism to control the parameter changes in the updating process, and they will often lead to an updated model of little physical meaning. Therefore, one of the fundamental questions in direct methods relates to the criteria of allowable changes in the initial stiffness and mass matrices. Some researchers, for example, Berman [2], Berman and Nagy [3], and Baruch [4] allowed any symmetrical changes in the matrices. The updated results were unsatisfactory because the connectivity between nodes is not correctly described and the updated matrices are fully populated. To keep the resemblance between the structure of the updated model and the structure of the real object, Kabe [5] and Caesar and Peter [6] confined the symmetrical changes to maintain the distribution of zero and non-zero elements only. Such changes avoided the above-mentioned problems, but still failed to keep the positive (semi-) definiteness of the matrices.

Among many parameter methods, sensitivity-based methods such as the inverse eigensensitivity method by Collins *et al.* [7] have proved very promising due to its stable performance in practical cases where measured co-ordinates are incomplete. This method was then improved by Lin *et al.* [8] to overcome the drawbacks in the assumption of small error magnitudes and slow speed of convergence. While these mathematical methodologies of model updating become well established, the selection of parameters remains a difficult problem of engineers. A popular approach exemplified by Chen and Graba [9] and Hoff and Natke [10] selects physical parameters to be adjusted, and keeps the assumed element shape functions unchanged. Thus, the updated model will have the correct definiteness and connectivity properties. In practice, however, this method is too restrictive because it carries the assumption that the initial model must exhibit all *effects* of the real structure, such as shear, bending, twisting, and their coupling. If the initial model neglects some of these effects, the method will fail to update the analytical model.

A new parameter selection strategy for finite element model updating was recently proposed by Gladwell and Ahmadian [11] and Ahmadian *et al.* [12], in which they introduce the concept of *generic* element stiffness and mass matrices. The model updating consists of two parts: defining the generic families of elements among which the "real" model exists; and finding the appropriate parameter values to specify the model in these families. In this way, the updated model obtained can predict the modal data well, and simultaneously satisfy the required positivity and connectivity conditions.

All civil engineering structures consist of connections or *joints* between the structural components. The various types of joints have significant effects on the static and dynamic behavior of the structures. Some experimental results [13] on assembled structures have shown that much of the flexibility and up to 90% of the damping are contributed by joints. The joints are fixed with different types of fasteners; bolts, welds, nails, screws and secondary components like angles, plates, gussets, and reinforcements. However, in practical analysis and design practice, only three types of framing joints are considered: (1) fully rigid joints; (2) perfectly pinned joints; (3) semi-rigid joints. Types I and II joints are well defined, and it is known to researchers that the former implies complete rotational continuity while the latter indicates no moment transfer. Yet, experimental investigation [14, 15] show that the true joint behavior is intermediate between these two simplified extremes and somewhat non-linear. A super-element model on the Tsing Ma Bridge deck has been constructed in the prediction of modal properties, and the differences between the analytical and experimental torsional modes [16] are always greater than those for the vertical and lateral transverse modes. This indicates that the flexibility of connecting joints of the bridge deck cannot be ignored. Therefore, a joint is often extremely difficult to model accurately using a purely analytical method, and a range of joint identification techniques have recently been proposed to correct the mathematical model of the joint from experimental data. A brief review of the joint identification method has been given by Ren [17].

Mottershead and Friswell [1] have discussed on the relationship between joint and the system identification problems, and they pointed out that the former is a special case of system identification. Nobari *et al.* [18] also compared the joint identification and model updating, and they drew the following conclusion: *although joint identification can be categorically considered as a special case of model updating since similar mathematical techniques can be used to tackle both problems, this does not imply that joint identification should be undertaken as part of model updating procedure since this is not a well-conditioned problem and adding the joints as further unknowns will worsen the situation.* Hence, they should be dealt with separately.

This paper presents the application of the generic element into a super-element model, and extends its usage into the join identification problem by selecting the stiffness of the semi-rigid joints as generic parameters, and they are updated simultaneously with other structural parameters. An experimental case study with a three-dimensional truss is used to illustrate the efficiency of the proposed method.

2. THEORY

2.1. STIFFNESS MATRIX OF A HYBRID FINITE ELEMENT WITH FLEXIBLE END JOINTS

The stiffness matrix of a hybrid finite element with flexible end joints can be obtained either by the stability function approach [19] or by the geometric stiffness approach [20]. The former has a more accurate relation between the axial force and the lateral deflection through iteration in solving the exact coupled differential equilibrium equations. This approach permits the use of one element to model one member in most cases. The latter includes the second order effects due to axial load, and it has the advantage of ease of formulation of the uncoupled equation. It does not require iterations to obtain an exact value for the axial force. But more than one element is needed to model a jointed member. Both methods can obtain an accurate solution and predict accurately the non-linear behavior of the flexible joint. However, both approaches are not appropriate for updating the initial finite element model, since the derived matrices are too complicated with too many unknowns in the model updating process which is not a well-conditioned problem itself. A simplified linear beam element with the flexible joint effects is proposed in this paper for model updating. The three-dimensional beam with semi-rigid joints at both ends is modelled by a beam element with three rotational springs at each end, as shown in Figure 1(a). The springs represent the bending or rotational stiffness about the three local axes. The initial modelling errors in the semi-rigid joints is limited to the fabrication and manufacturing defects which affect the flexibility of the group of joints.

Damping has been reported [21] to contribute to the modelling errors in a structure. The damping originating from a semi-rigid joint has been a research topic for many years, and no satisfactory formulation on its property has been developed which is suitable for parametric model updating. Therefore, this research is only on the model updating of stiffness characteristics of the joints.

Considering the set of springs belonging to a massless connection element between the beam and the joint as shown in Figure 1(b), the following equilibrium relations can be obtained for moments at the member ends:

$$\begin{bmatrix} K_1 & 0 & 0 \\ 0 & K_2 & 0 \\ 0 & 0 & K_3 \end{bmatrix} \begin{Bmatrix} \theta_1 \\ \theta_2 \\ \theta_3 \end{Bmatrix} = \begin{Bmatrix} M_1 \\ M_2 \\ M_3 \end{Bmatrix}, \tag{1}$$

in which

$$K_i = \begin{bmatrix} r_m^i & -r_m^i & 0 & 0 \\ -r_m^i & r_m^i + k_{11}^i & k_{12}^i & \\ & k_{21}^i & r_n^i + k_{22}^i & -r_n^i \\ & & -r_n^i & r_n^i \end{bmatrix}, \quad \theta_i = \begin{Bmatrix} {}_e\theta_m^i \\ {}_i\theta_m^i \\ {}_i\theta_n^i \\ {}_e\theta_n^i \end{Bmatrix}, \quad M_i = \begin{Bmatrix} {}_em_m^i \\ {}_im_m^i \\ {}_im_n^i \\ {}_em_n^i \end{Bmatrix}, \tag{2}$$

where $i = 1, 2\ 3$ denote the terms about the local x-, y- and z-axis, respectively, r_m, r_n are the joint stiffnesses at the two ends, written as $r^i = p/(1-p)(4EI/L)$ for $i = 2,\ 3$ and $r^1 = p(1-p)(GJ/L)$ in which p is the fixity factor, which will be zero for perfectly pinned joints and one for perfectly rigid joints, the second moment of inertia of the member cross-section about the x- and y-axis are assumed to be the same, ${}_e\theta_m^i$, ${}_e\theta_n^i$, ${}_i\theta_m^i$, and ${}_i\theta_n^i$ are, respectively, the external and internal rotation about the ith axis as shown in Figure 1(b), k_{pq}^i are the corresponding components of the stiffness matrix of a conventional beam

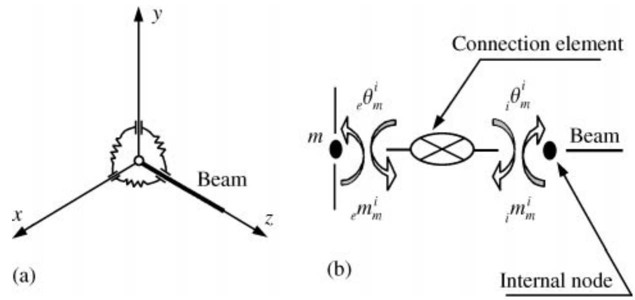

Figure 1. (a) Three-dimensional semi-rigid joint model; (b) Nomenclature at connection.

element if the bowing effect is ignored, given by

$$k^1_{pq} = \frac{GJ}{L}\begin{bmatrix} 1 & -1 \\ -1 & 1 \end{bmatrix}, \quad k^i_{pq} = \frac{EI}{L}\begin{bmatrix} 4 & 2 \\ 2 & 4 \end{bmatrix} \quad (i = 2,\ 3). \tag{3}$$

Since the external forces and moments are applied at the external nodes of the jointed member only, the applied moments about each axis at the internal nodes connecting the beam element and the spring can be obtained by considering equilibrium of the connection shown in Figure 1(b):

$$\begin{bmatrix} r^i_m + k^i_{11} & k^i_{12} \\ k^i_{21} & r^i_n + k^i_{22} \end{bmatrix}\begin{Bmatrix} {}_i\theta^i_m \\ {}_i\theta^i_n \end{Bmatrix} - \begin{bmatrix} r^i_m & 0 \\ 0 & r^i_n \end{bmatrix}\begin{Bmatrix} {}_e\theta^i_m \\ {}_e\theta^i_n \end{Bmatrix} = \begin{Bmatrix} 0 \\ 0 \end{Bmatrix} \quad (i = 1,\ 2,\ 3) \tag{4}$$

or

$$\begin{Bmatrix} {}_i\theta^i_m \\ {}_i\theta^i_n \end{Bmatrix} = \begin{bmatrix} r^i_m + k^i_{11} & k^i_{12} \\ k^i_{21} & r^i_n + k^i_{22} \end{bmatrix}^{-1}\begin{bmatrix} r^i_m & 0 \\ 0 & r^i_n \end{bmatrix}\begin{Bmatrix} {}_e\theta^i_m \\ {}_e\theta^i_n \end{Bmatrix} \quad (i = 1,\ 2,\ 3). \tag{5}$$

Substituting equation (5) into equation (1), the stiffness terms related to the internal nodes are eliminated, and the condensed stiffness matrix relating the moments and rotations about the external nodes can be written as

$$\begin{Bmatrix} {}_em^1_m \\ {}_em^2_m \\ {}_em^3_m \\ {}_em^1_n \\ {}_em^2_n \\ {}_em^3_n \end{Bmatrix} = \begin{bmatrix} K_{mn} & K_{21} \\ K_{12} & K_{nm} \end{bmatrix}\begin{Bmatrix} {}_e\theta^1_m \\ {}_e\theta^2_m \\ {}_e\theta^3_m \\ {}_e\theta^1_n \\ {}_e\theta^2_n \\ {}_e\theta^3_n \end{Bmatrix}, \tag{6}$$

where

$$K_{ij} = \begin{bmatrix} r^1_i - (r^1_i)^2(r^1_j + k^1_{22})/\rho_1 & 0 & 0 \\ 0 & r^2_i - (r^2_i)^2(r^2_j + k^2_{22})/\rho_2 & 0 \\ 0 & 0 & r^3_i - (r^3_i)^2(r^3_j + k^3_{22})/\rho_3 \end{bmatrix}$$

$$\text{for} \begin{Bmatrix} i = m,\ n \\ j = m,\ n \\ i \neq j \end{Bmatrix},$$

and

$$K_{12} = K_{21} = \begin{bmatrix} k_{12}^1 r_m^1 r_n^1/\rho_1 & 0 & 0 \\ 0 & k_{12}^2 r_m^2 r_n^2/\rho_2 & 0 \\ 0 & 0 & k_{12}^3 r_m^3 r_n^3/\rho_3 \end{bmatrix},$$

with

$$\rho_i = det\begin{bmatrix} k_{11}^i + r_m^i & k_{12}^i \\ k_{21}^i & k_{22}^i + r_n^i \end{bmatrix}. \tag{7}$$

Adding the terms for the axial force to equation (6), and transforming the resulting 8×8 matrix to the nodal d.o.f.s of the element, the stiffness matrix of the semi-rigid jointed beam element can be written as

$$K_e = T\begin{bmatrix} EA/L & 0 & 0 & 0 \\ 0 & K_{mn} & 0 & K_{21} \\ 0 & 0 & EA/L & 0 \\ 0 & K_{12} & 0 & K_{nm} \end{bmatrix}_{8\times 8} T^{\mathrm{T}}, \tag{8}$$

in which T is the 12×8 transformation matrix mapping the six external moments and two axial forces to the nodal forces and moments in the local co-ordinates, respectively, given by

$$T = \begin{bmatrix} 1 & 0 & 0 & 0 & 0 & 0 & 0 & 0 & 0 & 0 & 0 & 0 \\ 0 & 0 & 0 & 1 & 0 & 0 & 0 & 0 & 0 & 0 & 0 & 0 \\ 0 & 1/L & 0 & 0 & 1 & 0 & 0 & -1/L & 0 & 0 & 0 & 0 \\ 0 & 0 & 1/L & 0 & 0 & 1 & 0 & 0 & -1/L & 0 & 0 & 0 \\ 0 & 0 & 0 & 0 & 0 & 0 & 1 & 0 & 0 & 0 & 0 & 0 \\ 0 & 0 & 0 & 0 & 0 & 0 & 0 & 0 & 0 & 1 & 0 & 0 \\ 0 & 1/L & 0 & 0 & 0 & 0 & 0 & -1/L & 0 & 0 & 1 & 0 \\ 0 & 0 & 1/L & 0 & 0 & 0 & 0 & 0 & -1/L & 0 & 0 & 1 \end{bmatrix} \tag{9}$$

It can be easily verified that the semi-rigid jointed beam element expressed in equation (8) is equal to a pinned joint beam element if the spring stiffness is zero and equal to a rigid joint beam element if the spring stiffness is infinite.

2.2. SUPER-ELEMENT MODEL

The finite element models of modern civil engineering structures usually consist of a huge number of d.o.f.s. The number of analytical d.o.f.s will be much greater than the number of measured d.o.f.s. Although modal reduction [22] or modal expansion [23] techniques can be used to obtain the spatially incomplete modal data, both techniques will give rise to remarkable errors resulting in an ill-posed inverse problem with a large number of d.o.f.s. A super-element model has been developed in the damage assessment project of the Tsing Ma Bridge [24] to avoid this problem. The formulation of the bridge deck model of this

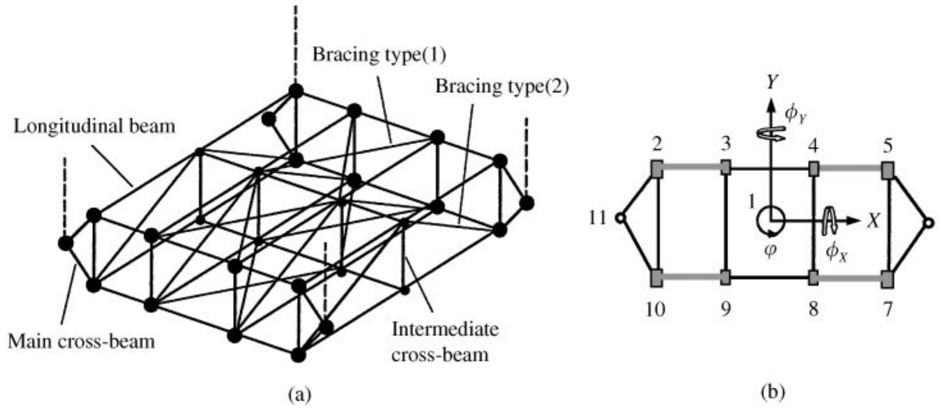

Figure 2. The super-element model for deck segment of the Tsing Ma Bridge.

long suspension bridge in Hong Kong is used in this paper for illustration of the super-element modelling.

The Tsing Ma Bridge is a long suspension bridge which serves as the link between the new airport of Hong Kong and the commercial centres. The bridge deck is a two-level enclosed structure, which carries a dual three-lane highway at the upper level and two railway tracks and two traffic lanes at the lower level. The whole deck structure can be divided into segments between adjacent sets of suspenders 18 m apart, the arrangement of which is shown in Figure 2(a). Each segment consists of 66 structural components of longitudinal beams, cross-beams, bracings and stiffened plates.

All the nodes of the super-element are allocated on the two outermost sections along the longitudinal axis. Each end section consists of a number of nodes and several sub-elements as shown in Figure 2(b), depending on the specific deck configuration. In the type of bridge deck under consideration, there are 10 master nodes and one slave node in the section. The primary longitudinal beams and auxiliary longitudinal beams are connected to nodes 2, 5, 7 and 10 and 3, 4, 8 and 9 respectively. Nodes 6 and 11 are at the intersection of cross-beams at the edges, and there are 14 cross-beams in the section, which are represented by the segments in the figure (the thicker lines indicate that there is also a stiffened plate between two adjacent longitudinal beams). Bracing members and stiffened plates are not shown in this figure since they are not in the same section. The 66 structural members are: eight longitudinal beams, 38 cross-beams, 16 bracing members and four stiffened plates modelled as four groups of sub-elements in the super-element. Nodes 3, 4, 8 and 9 each has three translational d.o.f.s parallel to the local co-ordinate axes. To take into account the rigidity of the triangular part enclosed by nodes 5, 6 and 7, it is assumed that these three nodes have the same translational d.o.f.s in the $X-Y$ plane, and each has one different translational d.o.f. in the longitudinal direction. A similar assumption is made for nodes 2, 10 and 11. In addition to the master nodal d.o.f.s, the slave node 1 possesses three d.o.f.s around the three global co-ordinate axes of the cross-section. Consequently, the model will have 25 d.o.f.s in one cross-section, and a total of 50 d.o.f.s in the super-element, whereas there will be more than 300 d.o.f.s if a standard three-dimensional finite element model is adopted. It is evident that the number of d.o.f.s will be significantly reduced by the use of this super-element.

The following paragraphs give the formulation of the contribution of one type of sub-element, i.e., the longitudinal beams, to the stiffness matrix of the super-element from the variational principle of minimum potential energy. Those from the cross-beams, bracing members and the stiffened plates are not presented.

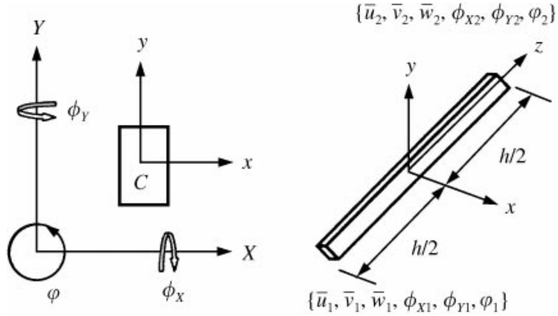

Figure 3. Longitudinal sub-element.

Figure 3 shows that the origin C of the longitudinal sub-element is seated at the center of gravity of the cross-section of the longitudinal beam. Let the three independent translational displacements of C be $\{\bar{u}, \bar{v}, \bar{w}\}^T$, and the global rotations of the super-element section around the X-, Y- and Z-axis be $\{\phi_X, \phi_Y, \varphi\}^T$, the deflections of an arbitrary point (x, y) in the beam section can be expressed as

$$u(x, y) = \bar{u} - \varphi(Y_C + y), \quad v(x, y) = \bar{v} + \varphi(X_C + x),$$
$$w(x, y) = \bar{w} + \phi_X(Y_C + y) - \phi_Y(X_C + x). \tag{10}$$

The strain in the z direction can be obtained as

$$\varepsilon_z = \frac{\partial w(x, y)}{\partial z} = \frac{d\bar{w}}{dz} - (X_C + x)\frac{d\phi_Y}{dz} + (Y_C + y)\frac{d\phi_X}{dz}$$
$$\gamma_{zx} = \frac{\partial w(x, y)}{\partial x} + \frac{\partial u(x, y)}{\partial z} = -\phi_Y + \frac{d\bar{u}}{dz} - (Y_C + y)\frac{d\varphi}{dz}, \tag{11}$$
$$\gamma_{zy} = \frac{\partial w(x, y)}{\partial y} + \frac{\partial v(x, y)}{\partial z} = \phi_X + \frac{d\bar{v}}{dz} + (X_C + x)\frac{d\varphi}{dz}.$$

Considering the longitudinal beam as a Timoshenko beam with two-way bending, its strain energy can be written as

$$H_{lb} = \frac{1}{2}\iiint(E\varepsilon_z^2 + G\gamma_{zx}^2 + G\gamma_{zy}^2)\,dz\,dx\,dy. \tag{12}$$

Substituting equation (11) into equation (12), and with some mathematical simplification, we have

$$H_{lb} = \frac{1}{2}\int\Bigg\{EA\Bigg[\left(\frac{d\bar{w}}{dz}\right)^2 + X_C^2\left(\frac{d\phi_Y}{dz}\right)^2 + Y_C^2\left(\frac{d\phi_X}{dz}\right)^2 - 2X_C\frac{d\bar{w}}{dz}\frac{d\phi_Y}{dz}$$
$$+ 2Y_C\frac{d\bar{w}}{dz}\frac{d\phi_X}{dz} - 2X_cY_C\frac{d\phi_X}{dz}\frac{d\phi_Y}{dz}\Bigg]$$
$$+ EI_Y\left(\frac{d\phi_Y}{dz}\right)^2 + EI_x\left(\frac{d\phi_X}{dz}\right)^2 - 2EI_{xy}\frac{d\phi_Y}{dz}\frac{d\phi_X}{dz}$$

$$+ GA\left[\phi_Y^2 + \phi_X^2 + \left(\frac{\mathrm{d}\bar{u}}{\mathrm{d}z}\right)^2 + \left(\frac{\mathrm{d}\bar{v}}{\mathrm{d}z}\right)^2 - 2\phi_Y\frac{\mathrm{d}\bar{u}}{\mathrm{d}z} + 2\phi_X\frac{\mathrm{d}\bar{v}}{\mathrm{d}z}\right.$$

$$\left. + 2Y_C\phi_Y\frac{\mathrm{d}\varphi}{\mathrm{d}z} + 2X_C\phi_X\frac{\mathrm{d}\varphi}{\mathrm{d}z} - 2Y_C\frac{\mathrm{d}\bar{u}}{\mathrm{d}z}\frac{\mathrm{d}\varphi}{\mathrm{d}z} + 2X_C\frac{\mathrm{d}\bar{v}}{\mathrm{d}z}\frac{\mathrm{d}\varphi}{\mathrm{d}z}\right]$$

$$\left. + G\left[A\left(X_C^2 + Y_C^2\right) + I_x + I_y\right]\left(\frac{\mathrm{d}\varphi}{\mathrm{d}z}\right)^2\right\}\mathrm{d}z, \tag{13}$$

where A is the cross-sectional area, I_x, I_y are the sectional moments of inertia of the beam cross-section with respect to the x- and y-axis, respectively, and $I_{xy} = \int xy\,\mathrm{d}A$. The deflections, i.e., $\bar{u}$, $\bar{v}$ of an arbitrary section along the longitudinal beam can be assumed in the form of a Hermite polynomial to include the contribution of bending modes:

$$\bar{u} = \bar{u}_1\left(\frac{1}{2} - \frac{3z}{2h} + \frac{2z^3}{h^3}\right) + \bar{u}_2\left(\frac{1}{2} + \frac{3z}{2h} - \frac{2z^3}{h^3}\right) + \phi_{Y1}h\left(\frac{1}{8} - \frac{z}{4h} - \frac{z^2}{2h^2} + \frac{z^3}{h^3}\right)$$

$$+ \phi_{Y2}h\left(-\frac{1}{8} - \frac{z}{4h} + \frac{z^2}{2h^2} + \frac{z^3}{h^3}\right), \tag{14}$$

where h is the length of the beam, and the subscripts 1 and 2 denote the values in the end sections of the super-element. The deflection $\bar{v}$ has a similar form as $\bar{u}$. However, the longitudinal deflection $\bar{w}$ may be assumed in a linear form:

$$\bar{w} = \bar{w}_1\left(\frac{1}{2} - \frac{z}{h}\right) + \bar{w}_2\left(\frac{1}{2} + \frac{z}{h}\right). \tag{15}$$

The global rotations of an arbitrary section $\{\phi_X, \phi_Y, \varphi\}^{\mathrm{T}}$ also take up the same linear form as for $\bar{w}$. Substituting these six shape functions in the forms of equations (14) and (15) into equation (13), the strain energy of the beam can be expressed in terms of the nodal displacements. After applying the second partial derivation of the strain energy with respect to the nodal displacements, we have the equilibrium equations as

$$\{F\}_{lb} = [K]_{lb}\{U\}_{lb} \quad \{U\}_{lb} = \{\bar{u}_1, \bar{v}_1, \bar{w}_1, \varphi_1, \phi_{X1}, \phi_{Y1}, \bar{u}_2, \bar{v}_2, \bar{w}_2, \varphi_2, \phi_{X2}, \phi_{Y2}\}^{\mathrm{T}}, \tag{16}$$

in which $\{U\}_{lb}$ is the nodal displacement vector, $\{F\}_{lb}$ is the nodal force vector, and the 12×12 matrix $[K]_{lb}$ is the stiffness matrix contribution of the longitudinal beam sub-element to the super-element.

2.3. SUPER-ELEMENT WITH SEMI-RIGID JOINTS

To take into account the effects of the flexible joints at the two ends of the longitudinal beam, the formulation in equations (1)–(8) can be repeated at the sub-element level. However, the components k_{pq}^i in the conventional stiffness matrix of a beam element should be replaced by the terms of the longitudinal beam sub-element, i.e.,

$$k_{pq}^1 = G(AX_C^2 + AY_C^2 + I_x + I_y)/h\begin{bmatrix} 1 & -1 \\ -1 & 1 \end{bmatrix}, \tag{17}$$

$$k_{pq}^2 = \begin{bmatrix} E(AY_C^2 + I_x)/h + GAh/3 & GAh/6 - E(AY_C^2 + I_x)/h \\ GAh/6 - E(AY_C^2 + I_x)/h & E(AY_C^2 + I_x)/h + GAh/3 \end{bmatrix}, \tag{18}$$

$$k_{pq}^3 = \begin{bmatrix} E(AX_C^2 + I_y)/h + GAh/3 & GAh/6 - E(AX_C^2 + I_y)/h \\ GAh/6 - E(AX_C^2 + I_y)/h & E(AX_C^2 + I_y)/h + GAh/3 \end{bmatrix}. \tag{19}$$

In addition, the mapping matrix T in equation (8) should also be reconstructed as

$$T^* = T\begin{bmatrix} 1 & 0 & 0 & 0 & Y_c & -X_c & 0 & 0 & 0 & 0 & 0 & 0 \\ 0 & 1 & 0 & -Y_c & 0 & 0 & 0 & 0 & 0 & 0 & 0 & 0 \\ 0 & 0 & 1 & X_c & 0 & 0 & 0 & 0 & 0 & 0 & 0 & 0 \\ 0 & 0 & 0 & 1 & 0 & 0 & 0 & 0 & 0 & 0 & 0 & 0 \\ 0 & 0 & 0 & 0 & 1 & 0 & 0 & 0 & 0 & 0 & 0 & 0 \\ 0 & 0 & 0 & 0 & 0 & 1 & 0 & 0 & 0 & 0 & 0 & 0 \\ 0 & 0 & 0 & 0 & 0 & 0 & 1 & 0 & 0 & 0 & Y_c & -X_C \\ 0 & 0 & 0 & 0 & 0 & 0 & 0 & 1 & 0 & -Y_c & 0 & 0 \\ 0 & 0 & 0 & 0 & 0 & 0 & 0 & 0 & 1 & X_c & 0 & 0 \\ 0 & 0 & 0 & 0 & 0 & 0 & 0 & 0 & 0 & 1 & 0 & 0 \\ 0 & 0 & 0 & 0 & 0 & 0 & 0 & 0 & 0 & 0 & 1 & 0 \\ 0 & 0 & 0 & 0 & 0 & 0 & 0 & 0 & 0 & 0 & 0 & 1 \end{bmatrix}. \tag{20}$$

2.4. MODEL UPDATING WITH GENERIC PARAMETERS SELECTION

Amongst the many existing mathematical approaches for model updating, the improved inverse eigensensitivity method (IIEM) [8] is used in the present study due to its stable performance and also because it does not require complete measured modal data. The specific eigenvalue and eigenvectors sensitivities for the rth mode are separately calculated by

$$\frac{\partial \lambda_r}{\partial p_k} = \{\phi_a\}_r^{\mathrm{T}} \frac{\partial [K]}{\partial p_k} \{\phi_x\}_r - (\lambda_x)_r \{\phi_a\}_r^{\mathrm{T}} \frac{\partial [M]}{\partial p_k} \{\phi_x\}_r, \tag{21}$$

$$\frac{\partial \{\phi\}_r}{\partial p_k} = \sum_{i=1;i\neq r}^{N} \frac{\{\phi_a\}_i \{\phi_a\}_i^{\mathrm{T}}}{(\lambda_x)_r - (\lambda_a)_i} \left[\frac{\partial [K]}{\partial p_k} - (\lambda_x)_r \frac{\partial [M]}{\partial p_k}\right] \{\phi_x\}_r - \frac{1}{2} \{\phi_a\}_r \{\phi_a\}_r^{\mathrm{T}} \frac{\partial [M]}{\partial p_k} \{\phi_x\}_r, \tag{22}$$

where p_k is the kth selected updating parameter, $[K]$ and $[M]$ are the stiffness and mass matrices of the whole structure, respectively, and the subscripts a and x denote the analytical and experimental values respectively.

After the improved eigenvalue and eigenvector sensitivities are computed, the model updating using the IIEM can be formulated as

$$\begin{bmatrix} \partial\lambda_1/\partial p_1 & \partial\lambda_1/\partial p_2 & \cdots & \partial\lambda_1/\partial p_H \\ \partial\{\phi\}_1/\partial p_1 & \partial\{\phi\}_1/\partial p_2 & \cdots & \partial\{\phi\}_1/\partial p_H \\ \vdots & \vdots & \vdots & \vdots \\ \partial\lambda_m/\partial p_1 & \partial\lambda_m/\partial p_2 & \cdots & \partial\lambda_m/\partial p_H \\ \partial\{\phi\}_m/\partial p_1 & \partial\{\phi\}_m/\partial p_2 & \cdots & \partial\{\phi\}_m/\partial p_H \end{bmatrix} \begin{Bmatrix} \Delta p_1 \\ \Delta p_2 \\ \vdots \\ \Delta p_H \end{Bmatrix} = \begin{Bmatrix} (\lambda_x)_1 - (\lambda_a)_1 \\ \{\phi_x\}_1 - \{\phi_a\}_1 \\ \vdots \\ (\lambda_x)_m - (\lambda_a)_m \\ \{\phi_x\}_m - \{\phi_a\}_m \end{Bmatrix}, \tag{23}$$

where H is the total number of selected updating parameters, and m modes are measured. Assuming that N is the number of measured co-ordinates, the total number of linear equations in equation (23) is $m \times (N+1)$, because each mode provides N equations from the measured mode shapes and one equation from the eigenvalue. An iterative procedure is used to solve the coupled equation (23) and to update the selected parameters p_i, because the eigensensitivities given by equations (21) and (22) are based on the first order approximation. Convergence is achieved when the Euclidean norm of the vector $\{\Delta p\}$ reaches a prescribed small value.

Although many mathematical approaches for model updating have been developed, the strategy for selecting updating parameters remains relatively new in this research area. For structures with a group of flexible joints, the usual and practical approach to the updating problem consists of the following two steps: update separate substructures without any joints, and then assemble them together and identify the joints. In this paper, the concept of *generic element* [12] is introduced into the proposed super-element model for the selection of updating parameters. All the structural variables at sub-element level and the characteristics of the semi-rigid joints are candidates for selection as the generic parameters, and they will be updated simultaneously in the computation.

The generic element is briefly described below. For an individual sub-element with z d.o.f.s, its free vibration is governed by

$$([K^{se}] - \lambda_i [M^{se}])\{\phi\}_i = 0, \quad i = 1, 2, \ldots, z, \tag{24}$$

where $[K^{se}]$, $[M^{se}]$ are the stiffness and mass matrices of the sub-element obtained above. If the sub-element has d rigid-body modes and $z-d$ strain modes, the modal shape matrix can be written in partitioned form as

$$[\Phi_0^{se}] = [\phi_1, \ldots, \phi_d | \phi_{d+1}, \ldots, \phi_z] = [\Phi_{0R}, \Phi_{0S}], \quad d \leqslant 6, \tag{25}$$

in which the supscript 0 denotes the initial value, and R and S denote *rigid-body* and *strain* modes respectively. It is assumed that an alternate set of modal vectors can be derived from the initial ones by $[\Phi^{se}] = [\Phi_0^{se}][S]^{-1}$, or

$$[\Phi_{0R} \;\; \Phi_{0S}] = [\Phi_R \;\; \Phi_S] \begin{bmatrix} S_R & S_{RS} \\ 0 & S_S \end{bmatrix} \tag{26}$$

in partitioned form, where $[S]$ is some non-singular matrix. This shows that the new rigid-body modes are linear combinations of the original ones, and their d number of rigid-body modes remain unchanged, while the new strain modes are combinations of all the original modes.

The modes of a sub-element are normalized with respect to $[M^{se}]$ and $[K^{se}]$, where

$$[M^{se}] = [\Phi^{se}]^{-\mathrm{T}}[\Phi^{se}]^{-1}, \quad [K^{se}] = [\Phi^{se}]^{-\mathrm{T}} \begin{bmatrix} 0 & 0 \\ 0 & \Lambda_S \end{bmatrix} [\Phi^{se}]^{-1}, \tag{27}$$

in which $[\Lambda_S]$ contains the eigenvalues of the strain modes on the leading diagonal. Substituting equation (26) into equation (27), and using the fact that $[\Phi_0^{se}]^{-\mathrm{T}} = [M_0^{se}][\Phi_0^{se}]$, we have

$$[M^{se}] = [M_0^{se}][\Phi_0^{se}][U][\Phi_0^{se}]^{\mathrm{T}}[M_0^{se}], \quad [K^{se}] = [M_0^{se}][\Phi_{0S}][V][\Phi_{0S}^{\mathrm{T}}][M_0^{se}], \tag{28}$$

in which $[U] = [S]^{\mathrm{T}}[S]$ and $[V] = [S_S^{\mathrm{T}}][\Lambda_S][S_S]$. If the modal data of a sub-element matrix is available, a continuous family of sub-elements among which the updated model is sought, can be defined by pre-defining the style of the matrices $[U]$ and $[V]$ on physical grounds and selecting their component parameters as updating parameters. In this way, we can take into account not only those effects we are aware of and not definite such as the semi-rigid joints, but also all the other effects that are accommodated in the generic family.

The longitudinal beam-type sub-element is taken again as an example. A symmetric plane is selected for the super-element as the perpendicular plane passing through the deck segment at midspan. All the modes of an individual longitudinal beam in the structure are governed by symmetry or asymmetry groups, and each partitioned matrix, i.e. $[S_R]$, $[S_{RS}]$, and $[S_S]$ [15] in equation (26) can be assumed to be diagonal [11]. Moreover, if the new model is supposed to represent a beam with the same mass and inertia moment as the initial one, $[S_R]$ would become the unity matrix $[I_d]$, and $[S]$ has the form

$$[S] = \begin{bmatrix} 1 & & & S_{1,7} & & \\ & \ddots & & & \ddots & \\ & & 1 & & & S_{6,12} \\ & & & S_7 & & \\ & & & & \ddots & \\ & & & & & S_{12} \end{bmatrix}_{12\times 12}. \tag{29}$$

Thus, we obtain $[U]$ and $[V]$ as

$$[U] = [S]^{\mathrm{T}}[S] = \begin{bmatrix} 1 & & & u_{1,7} & & \\ & \ddots & & & \ddots & \\ & & 1 & & & u_{6,12} \\ u_{1,7} & & & u_7 & & \\ & \ddots & & & \ddots & \\ & & u_{6,12} & & & u_{12} \end{bmatrix}_{12\times 12},$$

$$[V] = [S]^{\mathrm{T}}[\Lambda_S][S] = \begin{bmatrix} v_1 & & & \\ & v_2 & & \\ & & \ddots & \\ & & & v_6 \end{bmatrix}_{6\times 6}. \tag{30}$$

Consequently, there are 18 parameters (12 in matrix $[U]$, and 6 in matrix $[V]$) to be updated for all the longitudinal beam-type sub-elements with flexible joint effect in the generic element family.

Applying this generic strategy of selecting updating parameters to the IIEM mathematical model, the matrices of derivative in equations (21) and (22) can be calculated by

$$\frac{\partial[M]}{\partial p_k} = \sum_{i=1}^{L} \begin{bmatrix} 0 & & & \\ & \ddots & & \\ & & \dfrac{\partial[M_i^{se}]}{\partial p_k} & \\ & & & \ddots \\ & & & & 0 \end{bmatrix}, \quad \frac{\partial[K]}{\partial p_k} = \sum_{i=1}^{L} \begin{bmatrix} 0 & & & \\ & \ddots & & \\ & & \dfrac{\partial[K_i^{se}]}{\partial p_k} & \\ & & & \ddots \\ & & & & 0 \end{bmatrix}, \tag{31}$$

in which

$$\frac{\partial[M_i^{se}]}{\partial p_k} = [M_{0i}^{se}][\Phi_{0i}^{se}]\frac{\partial[U]}{\partial p_k}[\Phi_{0i}^{se}]^{\mathrm{T}}[M_{0i}^{se}],$$

$$\frac{\partial[K_i^{se}]}{\partial p_k} = [M_{0i}^{se}][\Phi_{0Si}^{se}]\frac{\partial[V]}{\partial p_k}[\Phi_{0Si}^{se}]^{\mathrm{T}}[M_{0i}^{se}], \tag{32}$$

where p_k are the selected generic parameters, and L is the number of sub-elements specified in the super-element model.

3. EXPERIMENT

3.1. THE EXPERIMENT

The different components of structural modelling and model updating are illustrated in an experiment. A modal test is performed in the laboratory on a three-dimensional 10-bay cantilevered truss structure which consists of prefabricated steel members and joints as shown in Figure 4. The truss members are steel tubes with a longitudinal dimension of 0·4 m, and the joints are interchangeable hollow balls connected to the members with steel bolts (Figure 5). The distance between the centres of two adjacent balls is exactly 0·5 m after fabrication of the truss. All the connection bolts are tightened with the same torsional moment to avoid asymmetry and non-linearities effects under the loading or vibration conditions. Table 1 summarizes the main material and geometrical properties of the components of the test structure.

The modal test was performed using a Link Dynamic System model 450 shaker and seven B & K 4371 piezoelectric accelerometers. A continuous random signal in the 0–100 Hz bandwidth was input by the shaker to the concrete pier at the fixed end of the truss. The horizontal and vertical transverse displacements were measured at each of the 40 joints through 16 sets of measurements. A total of 80 d.o.f.s were measured. The first set of measurements is from seven d.o.f.s selected evenly along the length of the truss. Their

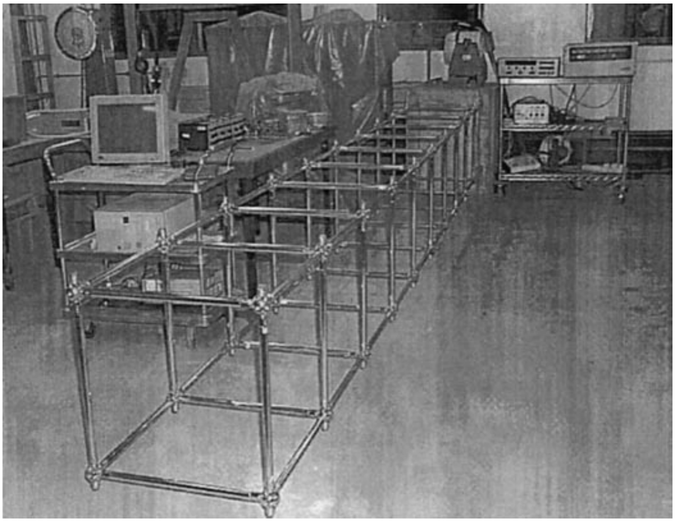

Figure 4. The 10-bay three-dimensional truss.

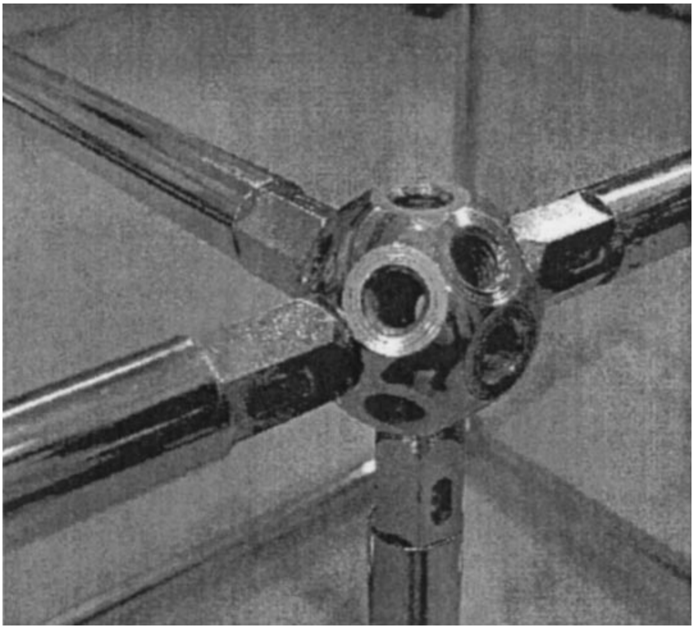

Figure 5. A joint of the truss.

TABLE 1

Material and geometrical properties of the test structure

Properties	Beam	Bolts	Balls
Young's modulus (N/m^2)	2·10E11	2·10E11	2·10E11
Area (m^2)	6·597E-5	—	—
Density (Kg/m^3)	1·2126E4	1·2126E4	1·2126E4
Mass (Kg)	0·32	0·09	0·23 + 0·072†
The Poisson ratio	0·3	0·3	0·3
Moment of inertia I_{xx} (m^4)	3·645E-9	—	—
Moment of inertia I_{yy} m^4)	3·645E-9	—	—
Torsional rigidity J (m^4)	7·290E-9	—	—

†Additional mass was added to each joint to balance the mass of the accelerometer.

responses will act as reference to the subsequent sets of measurements. Five other d.o.f.s were measured in each of the remaining sets of measurements with two of the reference d.o.f.s measured again. The measured mode shapes for the first 16 modes are shown in Figure 6. An additional mass was added to each joint to balance the effect of the moving accelerometers.

Modal analysis was performed on the initial analytical model to compare the results with those from the modal test of the real structure. The measured mode shapes exhibit a pattern of having two transverse modes followed by one torsional model. This pattern is repeated 4 times in the first 12 measured modes. However, the torsional modes are coupled with a severe warping effect, which can be easily noticed from the deformed 4-nodes cross-sections of the structure, as shown in Figure 7(a). The corresponding analytical mode shapes have cross-sections which remain in squares, as shown in Figure 7(b). It is evident

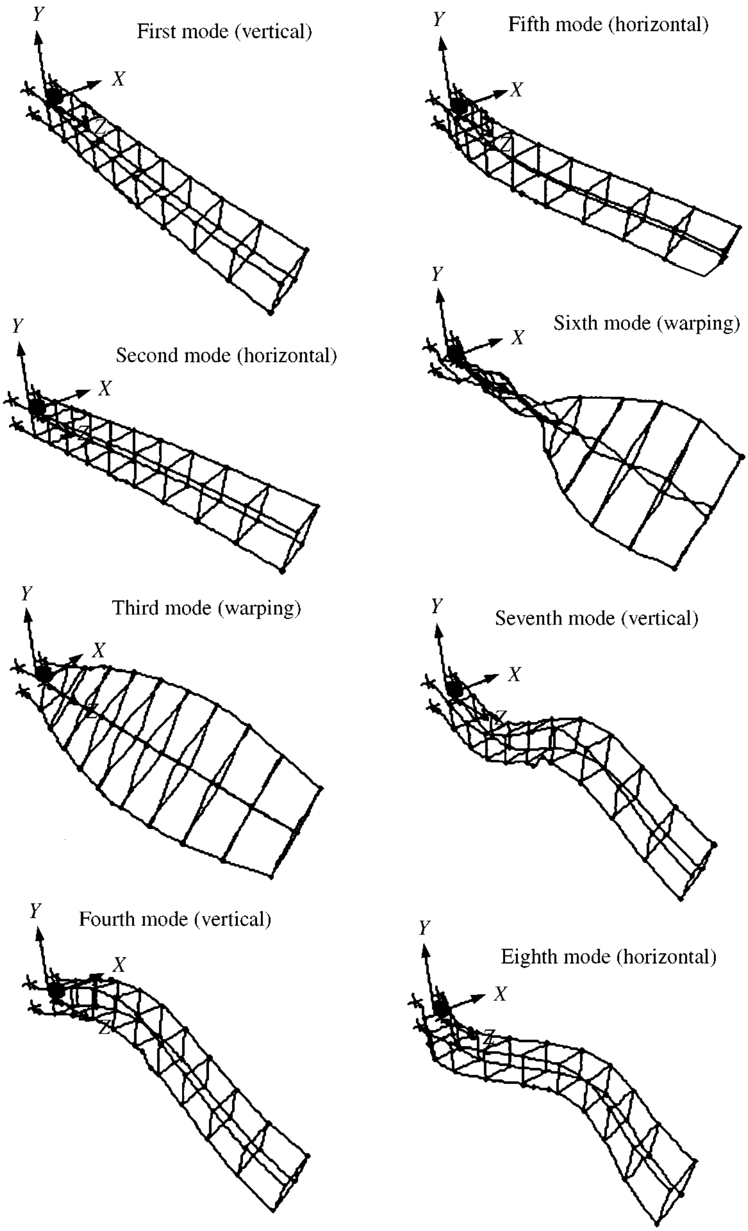

Figure 6. Measured mode shapes of the test structure.

that the flexible joint effect is significant in the test structure and it cannot be ignored. The same effect would also exist in the steel truss structure of the Tsing Ma Bridge deck.

3.2. THE SUPER-ELEMENT AND THE MODEL UPDATING

The super-element modelling technique with semi-rigid joints described in sections 2.2 and 2.3 is used to construct an analytical model for the test structure. The cantilevered 10-bay truss is divided into five super-elements in the longitudinal direction, each consists of

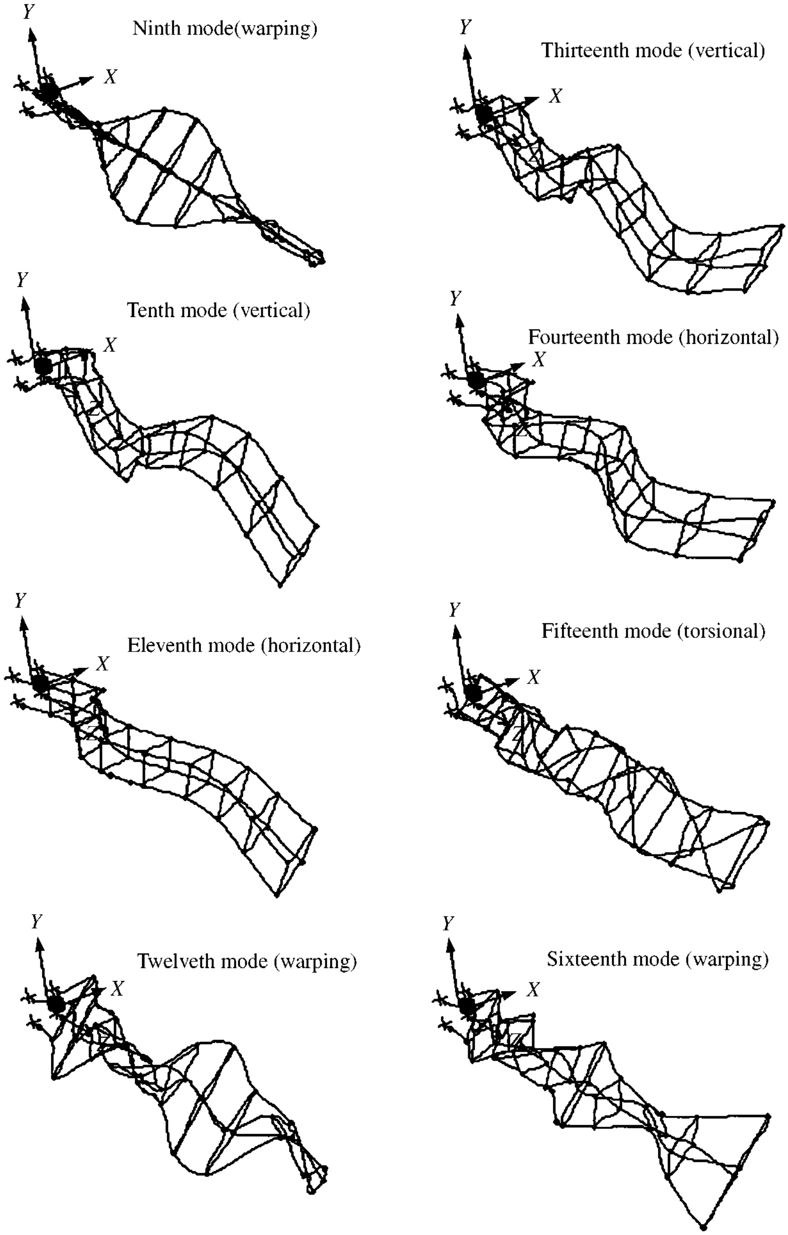

Figure 6. Continued.

four longitudinal beam-type sub-elements and 12 cross-beam-type sub-elements connected by semi-rigid joints. The super-element model of the beam segment is shown in Figure 8. There are four master nodes at the corners and one slave node at the centre of the end section. Each master node has three translational d.o.f.s parallel to the local co-ordinate axes. Each slave node has three rotational d.o.f.s about the three global axes of the end section. There are a total of 15 d.o.f.s in each end section, and there are 10 nodes (eight master and two slave) and 30 d.o.f.s for each super-element. Altogether there are 30 nodes and 75 d.o.f.s for the whole structure. This model is much smaller than the conventional

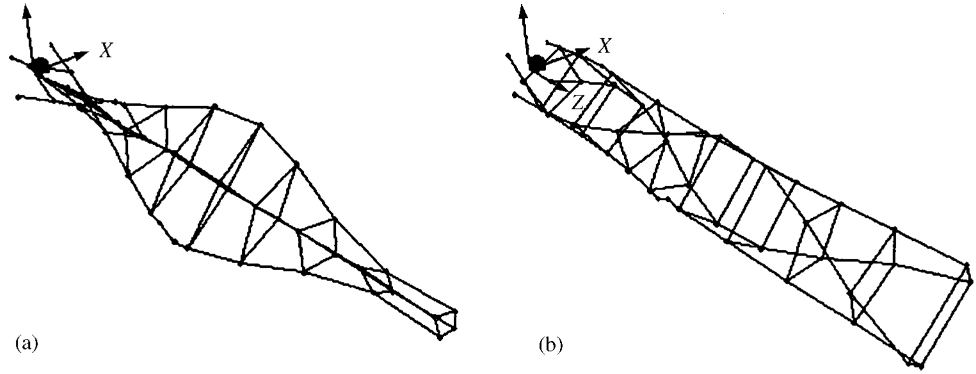

Figure 7. (a) Torsion and warping coupled mode of the test structure (ninth mode). (b) Pure torsional mode of the analytical model (ninth mode).

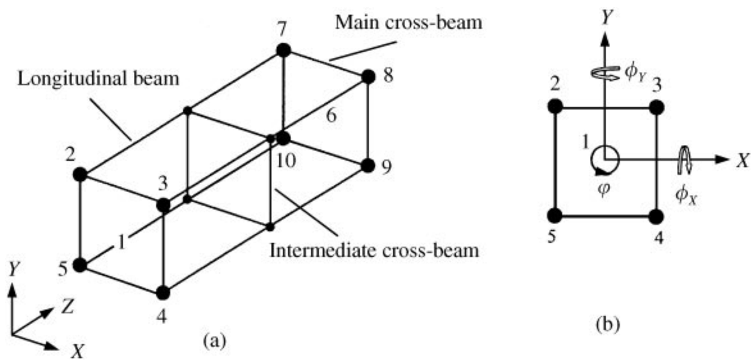

Figure 8. Super-element model of truss segment.

finite element model which has 240 d.o.f.s. For the initial structural model, the connection stiffness of the joints is assumed to be large by putting the fixity factor p equal to 0·9999, which implies very rigid joints connecting the members. The variation of the joint stiffness is plotted against the number of iterations in Figure 9. The fixity parameters r^1, r^2 and r^3 converge to 0·63, 0·85 and 0·80 respectively.

The experimental and analytical modal frequencies are compared. Figure 10(a) shows that the initial super-element model predicts the frequencies of the lower modes accurately and the differences increase and become noticeable as the mode order increases, especially for those torsional and warping coupled modes. Moreover, the analytical mode order is not consistent with the measured result for the higher modes starting from the ninth mode. There are only torsional modes in the analytical results, and the warping effects are not observed since the flexible joints in the analytical model are assumed to be perfectly rigid.

The differences in the natural frequencies and mode shapes can be attributed to two sources, (1) the super-element model ignores some physical effects by introducing the sectional d.o.f.s and condensing the stiffness (mass) relations of the sub-elements; and (2) more significantly, the behavior of the flexible joints cannot be described in the analytical model because of the perfectly rigid joint assumption.

The generic sub-element families for the longitudinal beam and cross-beam are defined, respectively, by equation (28), among which the true model exists and it can be sought by properly evaluating the selected generic parameters. Eighteen parameters are selected as

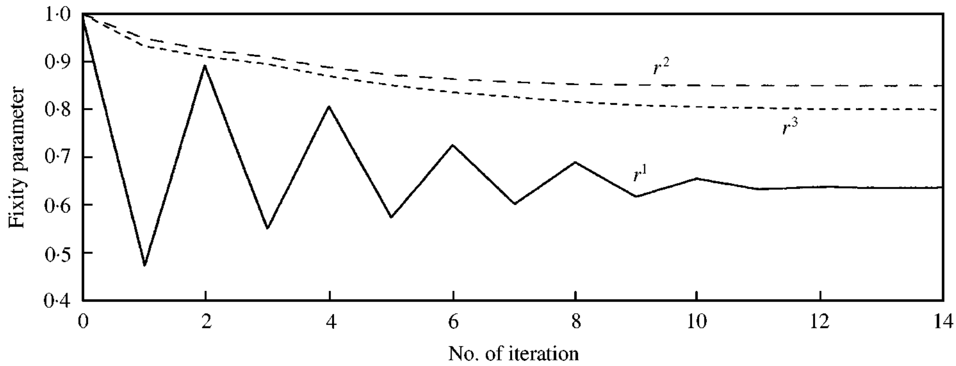

Figure 9. Convergence of fixity parameters r^1, r^2, r^3 of joints.

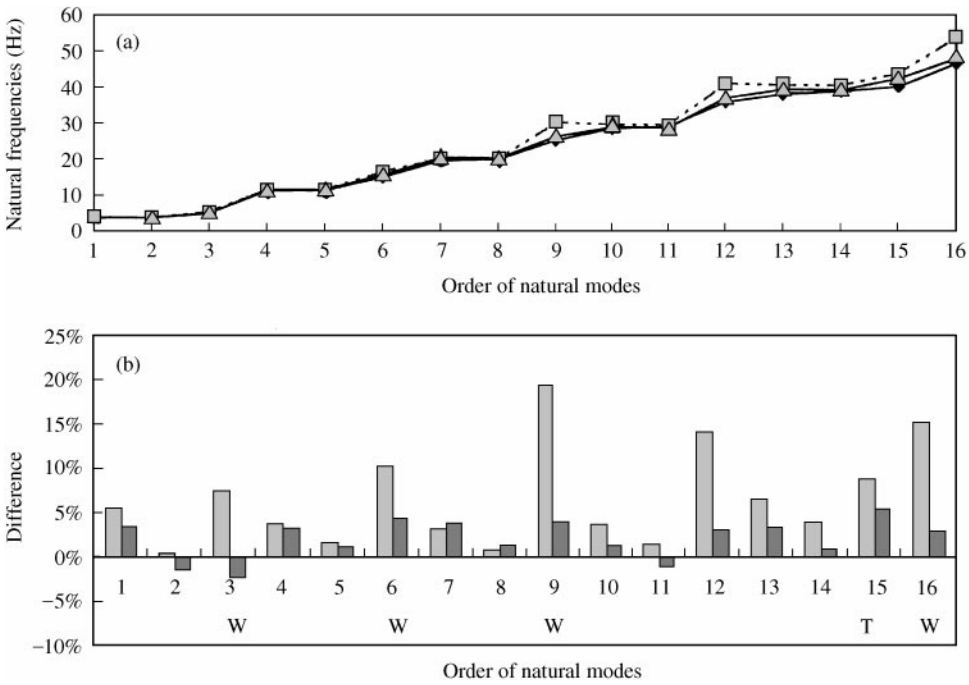

Figure 10. (a) Natural frequencies of the truss; —◆—, Test; ■ original SEM model; △, updated SEM model. (b) Difference in the natural frequencies between the analytical and experimental models (T—torsional mode; W—warping mode): ■, original SEM model; ■, updated SEM model.

illustrated in equation (30) to build a longitudinal beam generic family. However, 108 parameters are needed to define the cross-beam generic family since the sub-elements of this type lack the symmetry or asymmetry information on the super-element d.o.f.s. Although there are large number of sub-elements in the structural model, we can limit the number of unknown variables to an acceptable level by using the macroparameters shared by all the sub-elements of the same type. It is noted that the finite element model errors are not located in local parts in practice, but distributed spatially and widely in the whole structure. To further reduce the number of parameters, we can also consider the recommendations by Ross [25], to update only the dominant modes, i.e., higher modes of $[M^{se}]$ and lower modes of $[K^{se}]$ in equation (28), while keeping the others unchanged.

The IIEM approach is then used in the model updating process. The first 10 measured modes, excluding the third mode, are selected as the active modes. The third measured mode has some inconsistent phase information and is not used. Eigenvalue and eigenvector sensitivities of these modes are calculated by equations (21) and (22) to form the eigensensitivity matrix in equation (23). Those unmeasured elements of the modeshape vector $\{\phi_x\}_r$, which are the rotational d.o.f.s and the longitudinal translation d.o.f.s, are replaced by their analytical counterparts in the computation of the eigensensitivities. Consequently, there are altogether $9 \times (40 + 1)$ linear algebraic equations involved in the updating solution (40 equations from the measured d.o.f.s corresponding to the d.o.f.s of the super-element and one equation from the measured eigenvalue for each mode).

The updating results exhibit good correlation with the measured modal data as shown in Figures 10. The differences in the natural frequencies are significantly reduced not only at the nine active modes, but also at the higher passive modes with a maximum difference less than 6%. The incorrect mode order in the initial model is also corrected and consistent with the modal test result. This observation, as discussed by Keye (26), suggests that the modelling errors are fully corrected by the updating process and a refined model close to the real structure is obtained. Otherwise, the results will have a similar characteristic to that from the direct updating methods, which exactly repeat the test data at active modes but fail to predict the modal properties at higher passive modes.

The pure torsional mode numbers 3, 6, 9, 12 and 16 in the initial model are updated to become torsional modes coupled with warping effects, which are similar to those obtained from the experiment. Modal assurance criteria (MAC) are also calculated to check on the accuracy of the updated mode shapes. Table 2 lists the diagonal elements of the mass normalized MAC [21] between the measured modes and the analytical modes (initial and updated). It is seen that the MAC for the updated model have improvements over those from the initial model in all 16 modes. The values for the higher complex modes are relatively small which suggests that there are still some discrepancies between the updated model and the real structure.

TABLE 2

Diagonal elements of the mass normalized MAC

Mode	Measured frequency (Hz)	Initial MAC	Updated MAC
1	3·658	0·926	0·937
2	3·841	0·934	0·958
3	5·061	0·853	0·884
4	11·402	0·889	0·912
5	11·646	0·874	0·923
6	15·305	0·822	0·864
7	19·939	0·856	0·882
8	20·426	0·835	0·905
9	25·853	0·779	0·846
10	29·329	0·812	0·838
11	29·999	0·806	0·831
12	36·95	0·727	0·792
13	39·267	0·755	0·813
14	40·243	0·774	0·843
15	41·706	0·713	0·752
16	48·292	0·686	0·771

3.3. DISCUSSIONS

The super-element model can be used to achieve good updated results for the lower frequency modes but not for the higher frequency modes. A perfectly refined model that represents the real structure is not achieved, and the updated results have error which increases as the modal order increases. The first type of error is due to the incorrect assumptions made while condensing the finite element d.o.f.s to those of the super-element. The second type of error is from the difference in the macro updating parameter in different members resulting from different ways of assembling the test structure. But the more significant error comes from the incomplete measurement, particularly from the rotational d.o.f.s which cannot be measured in this study. Half of the d.o.f.s in a conventional finite element model of the truss are rotational d.o.f.s. The super-element model has the advantage that the rotational d.o.f.s are condensed and it has a smaller proportion of rotational d.o.f.s than the conventional finite element model. There are only 15 rotational d.o.f.s within a total of 75 d.o.f.s for the whole test structure. It is therefore considered that the use of all the lower mode shapes in the identification would reduce the first type of error while the other types of errors cannot be avoided.

4. CONCLUSIONS

This research addresses the problem on how to improve the structural model of a large engineering structure with semi-rigid joints using vibration measurement. The structure is modelled by different types of super-elements connected together with semi-rigid joints. Generic families of the elements are grouped together, and generic parameters of the structural system and the joint stiffnesses are selected as updating parameters. The system identification of the structure and joint identification can be performed simultaneously in an updating process The efficiency and accuracy of the model updating can therefore be improved significantly since the joint identification is carried out as part of the model updating process.

ACKNOWLEDGMENTS

The work described in this paper was supported by a grant from the Hong Kong Polytechnic University Research Funding Project No. S718.

REFERENCES

1. J. E. MOTTERSHEAD and M. I. FRISWELL 1993 *Journal of Sound and Vibration* **167**, 347–375. Model updating in structural dynamics: a survey.
2. A. BERMAN 1979 *AIAA Journal* **17**, 1147–1148. Mass matrix correction using an incomplete set of measured models.
3. A. BERMAN and E. J. NAGY 1983 *AIAA Journal* **21**, 1168–1173. Improvement of large analytical model using model test data.
4. A. BRAUCH 1984 *AIAA Journal* **22**, 561–563. Methods of reference basis for identification of linear dynamic structures.
5. A. M. KABE 1985 *AIAA Journal* **23**, 1431–1436. Stiffness matrix adjustment using modal data.
6. B. CAESAR and J. PETER 1987 *AIAA Journal* **25**, 1494–1499. Direct updating of dynamic mathematical models from model testing data.
7. J. D. COLLINS, G. C. HART, T. K. HASSELMAN and B. KENNEDY 1974 *AIAA Journal* **12**, 185–190. Statistical identification of structures.

8. R. M. LIN, M. K. LIM and H. DU 1995 *ASME Journal of Vibration and Acoustics* **117**, 192–198. Improved inverse eigensensitivity method for structural analytical model updating.
9. J. C. CHEN and J. A. GRABA 1980 *AIAA Journal* **12**, 684–690. Analytical model improvement using modal testing results.
10. C. HOFF and H. G. NATKE 1989 *The International Journal of Analytical and Experimental modal Analysis* **4**, 1–7. Correction of a finite element model by input–output measurements with application to a radar tower.
11. G. M. L. GLADWELL and H. AHMADIAN 1995 *Mechanical Systems and Signal Processing* **9**, 601–614. Generic element matrices suitable for finite element model updating.
12. H. AHMADIAN, G. M. L. GLADWELL and F. ISMAIL 1997 *ASME Journal of Vibration and Acoustics* **119**, 37–45. Parameter selection strategies in finite element model updating.
13. C. F. BEARDS 1986 *Shock and Vibration Digest* **17**, 17–19. Structural damping by slip in joints.
14. S. W. JONES, P. A. KERBY and D. A. NETHERCOT 1982 *Journal of Structural Engineering* **108**, 361–372. Columns with semi-rigid joints.
15. C. W. LEWITT, E. CHESSON and W. H. MUNSE 1969 *Engineering Bulletin of University of Illinois* 500. Restraint characteristics of flexible riveted and bolted beam-to-column connections.
16. "Lantau fixed crossing: wind and structural health monitoring masterplan Task 7.12—Report No. 3(a)—Finite element modelling and modal sensitivity analysis of the Tsing Ma Suspension Bridge." 1999 Department of Civil and Structural Engineering, Hong Kong Polytechnic University, Hung Hom, Kowloon, Hong Kong.
17. Y. REN 1992 *Ph.D. thesis, Imperial College of Science Technology and Medicine, London University, U.K.* The analysis and identification of friction joint parameters in the dynamic response of structures.
18. A. S. NOBARI, D. A. ROBB and D. J. EWINS 1993 *The International Journal of Analytical and Experimental Modal Analysis* **8**, 93–105. Model updating and joint identification methods: applications, restrictions and overlap.
19. E. M. LUI and W. F. CHEN 1987 *Computers and Structures* **26**, 719–732. Effects of joint flexibility on the behavior of steel frames.
20. P. P. T. CHUI and S. L. CHAN 1997 *Engineering Structures* **19**, 1001–1010. Vibration and deflection characteristics of semi-rigid jointed frames.
21. M. I. FRISWELL and J. E. MOTTERSHEAD 1995 *Finite Element Model Updating in Structural Dynamics*. Dordrecht: Kluwer Academic Publishers, chapter 4.
22. P. AVITABILE, F. PECHINSKY and J. O'CALLAHAN 1992 *10th International Modal Analysis Conference, San Diego, CA* 572–583. Study of vector correlation using various techniques for model reduction.
23. M. IMREGUN and D. J. EWINS 1983 *11th International Modal Analysis Conference, Kissimmee, FL* 168–175. An investigation into mode shape expansion techniques.
24. "Lantau fixed crossing: wind and structural health monitoring masterplan Task 7.12—Report No. 2 — Assessment strategy of possible structural damage in the Tsing Ma Bridge, Kap Shui Mun Bridge, and Ting Kau Bridge." 1998 Department of Civil and Structural Engineering, Hong Kong Polytechnic University, Hung Hom, Kowloon, Hong Kong.
25. R. G. ROSS 1971 *National Aeronautics and Space Engineering and Manufacturing Meeting, Society of Automotive Engineers, Los Angeles, CA*, 2627–2635. Synthesis of stiffness and mass matrices from experimental vibration modes.
26. S. KEYE 1997 *Proceedings of the Second International Conference on Identification of Engineering Systems*, 122–134. Prediction of modal and frequency response data from a validated finite element model.

APPENDIX A: NOMENCLATURE

r_m^i	the connection stiffness of joint m about the ith local axis
$[T]$	the mapping matrix to nodal displacement vector for conventional beam element
$[T^*]$	the mapping matrix to nodal displacement vector for longitudinal-beam-type sub-element
$[K^{se}]$	stiffness matrix of sub-elements
$[M^{se}]$	mass matrix of sub-elements
$[K]$	stiffness matrix for the structure
$[M]$	mass matrix for the structure

$[\Phi^{se}]$	mode shape matrix of sub-elements
$[\Lambda^{se}]$	eigenvalue matrix (diagonal) of sub-elements
$[\Phi_R]$	rigid-body mode shape matrix of sub-elements
$[\Phi_S]$	strain mode shape matrix of sub-elements
p_k	the kth selected generic parameter
$\partial\lambda_r/\partial p_k$	eigenvalue sensitivity for the rth mode
$\partial\{\phi\}_r/\partial p_k$	eigenvector sensitivities for the rth mode
$\partial[K]/\partial p_k$	the derived stiffness matrix with respect to p_k
$\partial[M]/\partial p_k$	the derived mass matrix with respect to p_k
$\partial[K_i^{se}]/\partial p_k$	the derived stiffness matrix of the ith sub-element with respect to p_k
$\partial[M_i^{se}]/\partial p_k$	the derived mass matrix of the ith sub-element with respect to p_k
λ_i	the ith eigenvalue of sub-elements
$\{\phi\}_i$	the ith eigenvector of sub-elements
$(\lambda_a)_i$	the ith eigenvalue of analytical model
$\{\phi_a\}_i$	the ith eigenvector of analytical model
$(\lambda_x)_r$	the rth eigenvalue of experimental model
$\{\phi_x\}_r$	the rth eigenvector of experimental model
$\{\Delta p\}$	vector of generic parameter changes
S	transfer matrix for generic sub-elements family
L	number of sub-elements specified in super-element model for the structure
N	number of d.o.f.s specified in super-element model for the structure
m	number of measured (active) modes
H	number of selected generic parameters
z	number of d.o.f.s specified in individual sub-element